

Strong gauge-boson scattering at LHC

Saurabh D. Rindani ^a

^a*Theoretical Physics Division
Physical Research Laboratory
Navrangpura, Ahmedabad 380009*

In the standard model with electroweak symmetry breaking through the Higgs mechanism, electroweak gauge-boson scattering amplitudes are large if the Higgs boson is heavy, and electroweak gauge interactions become strong. In theories with electroweak symmetry breaking through alternative mechanisms, there could be a strongly interacting gauge sector, possibly with resonances in an accessible energy region. In general, the scattering of longitudinally polarized massive gauge bosons can give information on the mechanism of spontaneous symmetry breaking. At energies below the symmetry breaking scale, the equivalence theorem relates the scattering amplitudes to those of the “would-be” Goldstone modes. In the absence of Higgs bosons, unitarity would be restored by some new physics which can be studied through WW scattering. Some representative models are discussed. Isolating WW scattering at a hadron collider from other contributions involving W emission from parton lines needs a good understanding of the backgrounds. Resonances, if they exist below about a TeV, would be feasible of observation at the LHC.

1. Introduction

The standard model (SM) of strong, electromagnetic and weak interactions is based on local gauge invariance under the group $SU(2)_L \times U(1) \times SU(3)_C$, spontaneously broken to $U(1)_{\text{em}} \times SU(3)_C$. The spontaneous breaking of gauge invariance gives masses to the gauge bosons W^\pm and Z corresponding to three of the generators of the gauge group in a way which maintains the renormalizability of the theory. The gauge bosons corresponding to the $U(1)_{\text{em}}$ gauge group of electromagnetism and the $SU(3)_C$ gauge group of colour remain massless. The spontaneous breaking is also required to give masses to the fermions in the theory.

Spontaneous symmetry breaking (SSB) in the SM is achieved by means of the Higgs mechanism. An $SU(2)_L$ doublet of spin-0 fields is present in the theory, and the configuration which minimizes the action corresponds to a nonzero value for the neutral component of the doublet. Thus, the ground state (vacuum state) of the theory is not invariant under the $SU(2)_L$ group, and the gauge symmetry is broken spontaneously. Since it is the neutral component of the scalar doublet which has a nonzero vacuum expectation value, $U(1)_{\text{em}}$ remains an unbroken symmetry.

As a result of SSB, three of the four degrees of freedom of the complex scalar doublet, get absorbed resulting in the longitudinal degrees of freedom of the (massive) gauge bosons. These are the so-called “would-be Goldstone” modes, since the Goldstone mechanism for a spontaneously broken *global* invariance would have required these modes to propagate as massless particles.

There remains one scalar field, the particle corresponding to which becomes massive. This massive spin-0 particle is known as the Higgs boson.

The introduction of spin-0 fields in the theory, while successful in breaking the electroweak gauge invariance to generate masses for gauge bosons and fermions, leads to certain problems. The main problem is that the mass of the Higgs boson cannot be made small in a natural way. As a result, alternative proposals have been considered for the mechanism of spontaneous symmetry breaking, some of which do not result in a light Higgs boson. The issue of the mechanism of spontaneous electroweak symmetry breaking is thus an important one. If the Higgs boson is discovered with properties predicted by SM, it would be a proof of Higgs mechanism. If the Higgs boson is not found, which would imply that it is either not present or very heavy, alternative mechanisms of SSB would have to be taken seriously.

The Large Hadron Collider (LHC) at CERN, Geneva, which in the very near future will collide protons on protons at a centre-of-mass energy of 14 TeV, is expected to unravel the mystery of the mechanism of SSB of the local gauge invariance responsible for the electroweak interactions. If the SM Higgs boson exists, and is light, it will be found. Alternatively, if the symmetry breaking is not due to a straightforward Higgs mechanism, or if the Higgs boson is not light, LHC should show other effects, particularly in scattering of weak gauge bosons. Scattering of longitudinally polarized weak bosons play a dominant role, and in the absence of a light Higgs boson, it is expected to become strong. Thus $W_L W_L$, $W_L Z_L$ and $Z_L Z_L$ scattering (where the subscript L de-

notes the longitudinal polarization mode), will be an important tool to study the mechanism of SSB.

Here we discuss the importance of studying gauge-boson scattering as a means of gaining knowledge about the electroweak symmetry breaking mechanisms, and also the feasibility of carrying out such a study at LHC. There have been a number of studies on strong gauge-boson scattering over the years. Since it is next to impossible to do an exhaustive review here, we will be forced to be selective.

We begin by discussing general features of scattering of massive spin-1 particles and specialize to the case when these particles are the gauge bosons of a spontaneously broken local gauge theory.

1.1. Longitudinal gauge-boson scattering

Amplitudes for scattering in theories with massive spin-1 particles can have bad high-energy behaviour. The propagator for a massive spin-1 field has a term which does not decrease with increasing momentum, leading to bad high-energy behaviour in amplitudes involving exchange of these vector particles. This can make the theory non-renormalizable. In theories with SSB, using the Higgs mechanism, renormalizability is maintained because Higgs exchange can cancel the bad high-energy behaviour arising from vector exchange. Amplitudes with massive vector particles in the initial and final states have bad high-energy behaviour because the polarization vector has the form

$$\epsilon_L^\mu(k) \approx \frac{k^\mu}{m_V}. \quad (1)$$

In the unitarity gauge, scattering of longitudinally polarized gauge bosons would have the largest amplitudes at high energy. In the high-energy limit, the amplitude for $W_L^+ W_L^-$ takes the form

$$\mathcal{M}^{\text{gauge}} = -\frac{g^2}{4m_W^2} u + \mathcal{O}((E/m_W)^0), \quad (2)$$

where u is the Mandelstam variable. Again, if the mass of the vector fields arises through a Higgs mechanism, the bad high-energy behaviour is cured. The contribution of s - and t - channel Higgs exchanges is

$$\begin{aligned} \mathcal{M}^{\text{Higgs}} &= -\frac{g^2}{4m_W^2} \left[\frac{(s-m_W^2)^2}{s-m_H^2} + \frac{(t-m_W^2)^2}{t-m_H^2} \right] \\ &\approx \frac{g^2}{4m_W^2} u, \end{aligned} \quad (3)$$

in the limit $s \gg m_H^2, m_W^2$, which cancels the bad high-energy behaviour of (2). However, if the Higgs mass is too high ($s \ll m_H^2$), the amplitude can be large, leading to a strongly-interacting gauge sector. The study of WW scattering can thus be important in studying

the mechanism of symmetry breaking. (Here, as well in what follows, we use WW to denote WW , WZ as well as ZZ combinations).

1.2. The equivalence theorem

Vector-boson scattering amplitudes at high energies may be calculated using the equivalence theorem [1]. The equivalence theorem relates the $W_L W_L$ scattering amplitude in the Feynman-'tHooft gauge to the amplitude for scattering of the corresponding ‘‘would-be’’ Goldstone scalars at high energy ($s \gg m_W^2$). Thus,

$$\begin{aligned} M(W_L W_L \rightarrow W_L W_L) &= M(w w \rightarrow w w) \\ M(Z_L Z_L \rightarrow Z_L Z_L) &= M(z z \rightarrow z z) \\ M(W_L Z_L \rightarrow W_L Z_L) &= M(w z \rightarrow w z) \\ M(W_L W_L \rightarrow Z_L Z_L) &= M(w w \rightarrow z z), \end{aligned} \quad (4)$$

where w and z are respectively the scalar modes which provide the longitudinal modes for W and Z respectively.

Goldstone boson interactions are governed by low-energy theorems for energy below the symmetry breaking scale ($s \ll m_{\text{SB}}^2$). Low-energy theorems are analogous to those obtained for $\pi\pi$ scattering in the chiral Lagrangian [2], and depend only on the symmetry of the theory. Thus, when there is no light Higgs (with $m_H < 1$ TeV or so), the low-energy theorems combined with equivalence theorem can predict $W_L W_L$ scattering amplitudes from the symmetries of the theory to leading order in s/m_{SB}^2 . The specific theory for symmetry breaking then shows up at the next higher order in s/m_{SB}^2 .

In the standard model (SM), we have the relations

$$m_H^2 = -2\mu^2 = 2\lambda v^2 = \lambda\sqrt{2}/G_F, \quad (5)$$

where λ is the quartic scalar coupling, and μ is the mass parameter in the scalar potential. v is the vacuum expectation value of the neutral Higgs. Since v and G_F are fixed from experiment, large m_H means large λ . For $\lambda \gtrsim 4\pi$, i.e., $m_H \gtrsim (4\pi\sqrt{2}/G_F)^{1/2}$, perturbation theory is not valid. This corresponds to $m_H \approx 1.2$ TeV.

1.3. Limit from unitarity

A limit may be obtained from unitarity, if the tree amplitudes are to be valid at high energies. In the absence of the Higgs, the amplitudes violate unitarity at high energies. The limit is of the order of the symmetry breaking scale. The Higgs cannot be very heavy, or else the unitarity limit would be crossed too soon. To see this, write the old-fashioned scattering amplitude f_{cm} , so that $|f_{cm}|^2 = \frac{d\sigma}{d\Omega}$. Then we have

$$f_{cm} = \frac{1}{8\pi\sqrt{s}} \mathcal{M}. \quad (6)$$

The scattering amplitude has the partial wave expansion

$$f(\theta) = \frac{1}{k} \sum_l (2l+1) P_l(\cos\theta) a_l, \quad (7)$$

where $a_l = e^{i\delta_l} \sin \delta_l$ is the partial wave amplitude written in terms of the phase shift δ_l . Unitarity is expressed by the optical theorem relation

$$\sigma = (4\pi/k) \text{Im}f(0). \quad (8)$$

For elastic scattering, the phase shift δ_l is real, but has a positive imaginary part if there is inelasticity. A convenient way to express elastic unitarity is

$$\text{Im}[a_l^{-1}] = -1. \quad (9)$$

From this it follows that

$$|a_l| \leq 1; \quad |\text{Re} a_l| \leq \frac{1}{2}. \quad (10)$$

The $l = 0$ partial-wave unitarity for large s for WW scattering then gives, in the absence of the Higgs boson,

$$\text{Re} a_0 \equiv \text{Re} \frac{G_F s}{16\pi\sqrt{2}} < 1/2. \quad (11)$$

Thus, for large enough s , unitarity is violated. The best bound comes from the isospin zero channel $\sqrt{1/6}(2W_L^+W_L^- + Z_L Z_L)$, viz.,

$$s < \frac{4\pi\sqrt{2}}{G_F} \approx (1.2 \text{ TeV})^2. \quad (12)$$

In the case of the standard Higgs mechanism, unitarity is restored by the exchange of a light Higgs boson. For unitarity to hold in the presence of the Higgs boson, the mass of the Higgs boson should satisfy

$$m_H^2 < \frac{4\sqrt{2}\pi}{G_F}. \quad (13)$$

This gives a limit of $m_H < 1.2$ TeV. Similar limits may be obtained by considering other partial-wave channels.

If there is no light Higgs, the perturbative unitarity limit is violated, and the gauge interactions are no longer weak. We then have a strong gauge sector. This could lead to the possibility of strong-interaction resonances, as seen in the case of the usual hadrons.

We will now discuss scenarios beyond the standard Higgs mechanism, where either there is no light Higgs, or the Higgs sector is more complicated than that in SM, so that the WW scattering can become strong.

2. $W_L W_L$ scattering beyond Higgs mechanism

As we have seen, absence of a light Higgs boson leads to violation of unitarity. Violation of unitarity may be prevented, or postponed to higher energy, in different ways, depending on the model. Models can have extra fermions and extra gauge interactions, which give additional contributions to $W_L W_L$ scattering, e.g., resonances. An important consideration for many of the theories with a modified electroweak symmetry-breaking mechanism is conformity with precision tests. Specifically, they can have an unacceptably large S parameter of the oblique parameters S, T, U proposed by Peskin and Takeuchi [3], and a negative contribution to S is needed to restore agreement with experiment.

It is necessary to discriminate among mechanisms which give new effects in WW scattering. In particular, their treatment would be different depending on whether the gauge interaction remains perturbative or not. One possibility is that of a heavy Higgs, $m_H \gg m_W^2$. In such a case, WW scattering would become large until the Higgs pole is crossed. If the Higgs mass is above the unitarity limit, the gauge-boson interaction becomes non-perturbative. This needs special non-perturbative treatment of gauge-boson interactions, and it is possible that the strong interaction produces resonances which would be seen. The second possibility is that there is no Higgs boson, and the symmetry is broken dynamically. In such a case there is a new sector with strong interactions, and this could produce its own resonances. A third possibility is that there is a light Higgs in an extension of the standard model. Then again two cases arise: One where there are other Higgs bosons, and the dynamics still remains perturbative for WW centre-of-mass energy beyond the light Higgs resonance until the other Higgs resonances are crossed, or could become strong if the remaining Higgs bosons are heavy. These possibilities are discussed in the context of two-Higgs doublet models in [4, 5]. The other case is when the light Higgs is light because it is a pseudo-Goldstone boson of a higher global symmetry, broken by the SM interactions [6]. In either case, WW scattering would be interesting to study in spite of a light Higgs boson.

We discuss a few of these models below. However, we begin with a model-independent approach.

2.1. Electroweak Chiral Lagrangian

In view of the variety of models, it would be preferable to have a unified, model-independent description of $W_L W_L$ scattering. Effective Lagrangians may be used to provide such a description, valid up to a certain cut-off Λ . A no-resonance scenario is described in

an electroweak chiral Lagrangian (EWCL) model, where one writes effective bosonic operators [7] in a series of increasing dimensions. The coefficients will have inverse powers of Λ . The effective Lagrangian is a low-energy expansion, and at the lowest non-trivial order, corresponding to operators of the lowest dimension, the scattering amplitudes for longitudinal gauge bosons, on using the equivalence theorem, would satisfy the low-energy theorems. However, coefficients of the higher-dimensional operators have to be fixed either on the basis of some underlying theory, or, in a purely phenomenological approach, from experiment.

Since the chiral Lagrangian is valid at low energies, an extrapolation to higher energies would lead to violation of unitarity. Unitarization can be built in in a somewhat *ad hoc* fashion by the use of Padé approximants, also known as the Inverse Amplitude Method (IAM), or the K-matrix method and this can generate a resonant behaviour [8]. The N/D method, developed for strong interactions [9], has also been applied for unitarization of electroweak amplitudes [10].

Terms in the chiral Lagrangian must respect $SU(2)_L \times U(1)$ gauge symmetry, which is broken spontaneously. Experimental constraints require that the Higgs sector also approximately respect a larger $SU(2)_L \times SU(2)_C$ symmetry, where the second factor $SU(2)_C$ corresponds to the so-called custodial symmetry. The custodial symmetry is broken by the Yukawa couplings and the $U(1)$ gauge couplings. The global symmetry could in principle be even larger.

The chiral Lagrangian is thus constructed using the dimensionless unitary unimodular matrix field $U(x)$, which transforms under $SU(2)_L \times SU(2)_C$ as $(2, 2)$. This corresponds to a non-linear realization of the symmetry. $U(x)$ may be represented in terms of real (would-be Goldstone) fields π_a , ($a = 1, 2, 3$), as follows:

$$U(x) = \exp \frac{i}{v} \sum_{a=1}^3 \pi_a \tau_a, \quad (14)$$

where τ_a , $a = 1, 2, 3$, are the usual 2×2 Pauli matrices, and v is the symmetry breaking scale¹.

The covariant derivative of $U(x)$ is

$$D_\mu U = \partial_\mu U + ig \frac{\vec{\tau}}{2} \cdot \vec{W}_\mu U - ig' U \frac{\tau_3}{2} B_\mu. \quad (15)$$

Further, the basic building blocks which are $SU(2)_L$ covariant and $U(1)_Y$ invariant are

$$T \equiv U \tau_3 U^\dagger, \quad V_\mu \equiv (D_\mu U) U^\dagger, \quad (16)$$

¹These π_a should not be confused with the π -meson fields. The w, z scalar fields, corresponding to the longitudinal polarization modes of the gauge bosons W, Z , are linear combinations of the π_a .

$$W_{\mu\nu} \equiv \partial_\mu W_\nu - \partial_\nu W_\mu + ig[W_\mu, W_\nu] \quad (17)$$

where T, V_μ and $W_{\mu\nu}$ have dimensions zero, one, and two respectively.

Terms in the chiral Lagrangian in the $M_H \rightarrow \infty$ limit of the linear theory at tree level are:

$$\begin{aligned} \mathcal{L}_0 = & \frac{1}{4} v^2 \text{Tr}[(D_\mu U)^\dagger (D^\mu U)] \\ & - \frac{1}{4} B_{\mu\nu} B^{\mu\nu} - \frac{1}{2} \text{Tr} W_{\mu\nu} W^{\mu\nu}, \end{aligned} \quad (18)$$

where v is the symmetry breaking scale and $B_{\mu\nu} \equiv \partial_\mu B_\nu - \partial_\nu B_\mu$. The first term has dimension two, while the second two (kinetic energy) terms have dimension four. The gauge couplings to the quarks and leptons must also be added. The Yukawa couplings of the quarks and leptons should also be included in the symmetry breaking sector.

An additional dimension-two operator is allowed by the $SU(2)_L \times U(1)$ symmetry:

$$\mathcal{L}'_1 = \frac{1}{4} \beta_1 g^2 v^2 [\text{Tr}(TV_\mu)]^2. \quad (19)$$

This term does not emerge from the $M_H \rightarrow \infty$ limit of the renormalizable theory at tree level. It violates the $SU(2)_C$ custodial symmetry even in the absence of the gauge couplings. It is the low-energy description of custodial-symmetry breaking physics which has been integrated out, at energies above roughly $\Lambda \equiv 4\pi v \simeq 3$ TeV. At tree level, \mathcal{L}'_1 contributes to the deviation of the ρ parameter from unity.

At the dimension-four level, there are a variety of new operators that can be written down. Making use of the equations of motion, and restricting attention to CP-invariant operators, the list can be reduced to eleven independent terms [7]:

$$\begin{aligned} \mathcal{L}_1 &= \frac{1}{2} \alpha_1 g g' B_{\mu\nu} \text{Tr}(TW^{\mu\nu}) \\ \mathcal{L}_2 &= \frac{1}{2} i \alpha_2 g' B_{\mu\nu} \text{Tr}(T[V^\mu, V^\nu]) \\ \mathcal{L}_3 &= i \alpha_3 g \text{Tr}(W_{\mu\nu} [V^\mu, V^\nu]) \\ \mathcal{L}_4 &= \alpha_4 [\text{Tr}(V_\mu V_\nu)]^2 \\ \mathcal{L}_5 &= \alpha_5 [\text{Tr}(V_\mu V^\mu)]^2 \\ \mathcal{L}_6 &= \alpha_6 \text{Tr}(V_\mu V_\nu) \text{Tr}(TV^\mu) \text{Tr}(TV^\nu) \\ \mathcal{L}_7 &= \alpha_7 \text{Tr}(V_\mu V^\mu) \text{Tr}(TV_\nu) \text{Tr}(TV^\nu) \\ \mathcal{L}_8 &= \frac{1}{4} \alpha_8 g^2 [\text{Tr}(TW_{\mu\nu})]^2 \\ \mathcal{L}_9 &= \frac{1}{2} i \alpha_9 g \text{Tr}(TW_{\mu\nu}) \text{Tr}(T[V^\mu, V^\nu]) \\ \mathcal{L}_{10} &= \frac{1}{2} \alpha_{10} [\text{Tr}(TV_\mu) \text{Tr}(TV_\nu)]^2 \\ \mathcal{L}_{11} &= \alpha_{11} g \epsilon^{\mu\nu\rho\lambda} \text{Tr}(TV_\mu) \text{Tr}(V_\nu W_{\rho\lambda}) \end{aligned} \quad (20)$$

The EWCL incorporates the low-energy theorems, and therefore the piece \mathcal{L}_0 is completely fixed in terms of the symmetry-breaking scale v . However, the coefficients of the higher-dimensional operators have to be

determined from experiment. Alternatively, they can be matched with a suitable underlying theory of one's choice.

The pieces of the EWCL contributing to gauge-boson two-point functions have been tested in precision tests, and these contribute to the oblique parameters, S , T and U [3]. \mathcal{L}'_1 , \mathcal{L}_1 and \mathcal{L}_8 are directly related to the S , T and U parameters. By setting the Goldstone boson fields to zero in these operators, which is equivalent to going to the unitarity gauge, we get

$$S \equiv -16\pi \frac{d}{dq^2} \Pi_{3B}(q^2)|_{q^2=0} = -16\pi\alpha_1, \quad (21)$$

$$\alpha T \equiv \frac{e^2}{c^2 s^2 m_Z^2} (\Pi_{11}(0) - \Pi_{33}(0)) = 2g^2\beta_1, \quad (22)$$

$$U \equiv 16\pi \frac{d}{dq^2} [\Pi_{11}(q^2) - \Pi_{33}(q^2)]|_{q^2=0} = -16\pi\alpha_8. \quad (23)$$

The $\Delta\rho(\equiv\rho-1)$ parameter is related to T by $\Delta\rho_{new} = \Delta\rho - \Delta\rho_{SM} = \alpha T$, where $\Delta\rho_{SM}$ is the contribution arising from standard model corrections.

These relations have been used in [11] to study the possible values of the EWCL coefficients in the presence of a SM Higgs boson with a mass larger than the electroweak precision measurement limits. They find the following 68% CL allowed ranges for S and T , which could be converted to the ranges for the parameters α_1, β_1 using the eqns. (21) and (22) above:

$$-0.37 < S < -0.17, \quad 0.34 < T < 0.58 \quad (24)$$

The smallness of the parameter T can be understood in terms of the approximate $SU(2)_C$ custodial symmetry. This approximate symmetry implies that the coefficients $\alpha_{2,6,7,8,9,10,11}$ will be sub-dominant relative to the custodial-symmetry preserving ones. Gauge-boson scattering can be considered to be dominated by the two coefficients α_4 and α_5 .

There are constraints from unitarity, analyticity and causality of scattering amplitudes on the effective Lagrangian parameters [12, 13]. The requirement of unitarity of the theory forces the cutoff of the EWCL to be about $\Lambda < 1.2$ TeV, but does not impose any constraints on the coefficients α_i, β_1 . Causal and analytical structure of the amplitudes leads to bounds on the possible values of α_4 and α_5 . These were first obtained in the context of chiral Lagrangians for strong interactions [14], and have been extended to the electroweak case. The second derivative with respect to the centre-of-mass energy of the forward elastic scattering amplitude of two Goldstone bosons is bounded from below by

a positive integral of the total cross section for the transition $2\pi \rightarrow \text{all}$ [12]. However, it was shown by Vecchi [13] that stronger bounds are obtained from causality (we refer the reader to [13] for details):

$$\alpha_4(\mu) \geq \frac{1}{12(4\pi)^2} \ln \frac{\Lambda^2}{\mu^2}, \quad (25)$$

$$\alpha_4(\mu) + \alpha_5(\mu) \geq \frac{1}{8(4\pi)^2} \ln \frac{\Lambda^2}{\mu^2}. \quad (26)$$

Fig. 1, taken from [15] shows the allowed regions in the plane of α_4 and α_5 after including constraints from causality and indirect bounds from precision experiments. The figure also includes a ‘‘black box’’, the region inaccessible at LHC (see below).

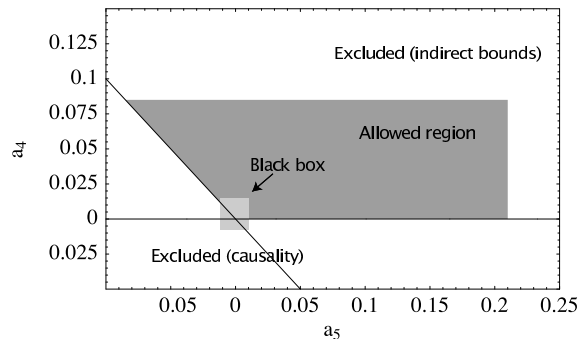


Figure 1. The region of allowed values in the $\alpha_4 - \alpha_5$ plane ($a_4 - a_5$ plane, in the notation of [15]), combining indirect bounds and causality constraints, is shown in gray. Also depicted is the region below which LHC will not be able to resolve the coefficients (‘‘black box’’). (From [15]).

Further constraints on the parameters can be obtained from triple and quartic gauge boson couplings through direct experimental measurement. The quartic couplings, which correspond to gauge-boson scattering, were studied in the LHC context in [16, 17], where the second reference cited considered six-fermion final states at orders α_{em}^6 and $\alpha_{em}^4 \alpha_s^2$. It was found in [17] that with an integrated luminosity of 100 fb^{-1} , LHC could place the following 99% CL bounds on the EWCL parameters α_4, α_5 :

$$-7.7 \times 10^{-3} < \alpha_4 < 15 \times 10^{-3}, \quad (27)$$

$$-12 \times 10^{-3} < \alpha_5 < 10 \times 10^{-3}. \quad (28)$$

These bounds correspond to assuming one parameter nonzero at a time.

In EWCL, one can build in unitarity at a given order by using a non-perturbative modification, which reduces to the original amplitude at the perturbative level [8]. One writes a low-energy expansion as $a(s) = a^{\text{LET}}(s) + a^{(1)}(s)$, where a^{LET} represents the amplitude given by the low-energy theorems. At the lowest order the Padé approximant gives

$$a^{\text{Pade}}(s) = \frac{a^{\text{LET}}(s)}{1 - \frac{a^{(1)}(s)}{a^{\text{LET}}(s)}}. \quad (29)$$

The K matrix method, which is simpler, consists in multiplying the amplitude by $-i$ and adding it to the denominator, so that the condition $\text{Im } a^{-1}$ is satisfied. It gives

$$a^K(s) = \frac{a^{\text{LET}}(s) + \text{Re}a^{(1)}(s)}{1 - i(a^{\text{LET}}(s) + \text{Re}a^{(1)})}. \quad (30)$$

Both satisfy unitarity by construction to the relevant order.

A recent suggestion [18] has been to add resonances to the EWCL, in appropriate isospin channels so as to preserve custodial $SU(2)$ symmetry, parametrizing them simply by their masses and widths. Ref. [18] uses a simple K matrix unitarization. With an appropriate off-shell extension of the interactions, the authors have implemented the process of WW scattering in an event generator for six final-state fermions, it viz., WHIZARD [19].

2.2. Technicolor models

Technicolor models are of the earliest proposals for dynamical breaking of the electroweak symmetry [20], without the introduction of elementary scalar fields. In analogy with QCD, local $SU(N)$ gauge invariance among technifermions in the fundamental representation leads to condensates which act as effective scalar fields and are responsible for breaking of the electroweak symmetry. The relevant coupling in technicolor theories is scaled up as compared to QCD to account for the electroweak scale. Thus, scattering of longitudinal gauge bosons can be strong.

The basic problem with technicolor, even when ordinary fermions acquire mass via an extended technicolor (ETC) sector [21], is that of large flavour-changing neutral currents and a large contribution to the S parameter. A proposal to address this problems has been walking technicolor (WT) [22] (in contrast to the usual theories which have renormalization group “running”). Walking dynamics helps suppressing flavour-changing neutral currents without preventing ETC from yielding realistic fermion masses. Certain WT models are

also in agreement with constraints imposed by precision electroweak data [23], because of the fact that walking dynamics itself can lower the contribution to the S parameter compared to a running theory. Various other modifications of WT theories have been considered recently to address different problems, and it seems that it is possible to construct working models of WT.

The scattering of Goldstone bosons representing the longitudinal gauge bosons was examined recently in [24, 15]. In [24], the authors examine to what extent the violation of unitarity in WW scattering can be delayed in the case of a realistic WT model which satisfies existing phenomenological constraints. They consider three scenarios with values of the oblique parameter S 0.1, 0.2 and 0.3. Making use of Weinberg sum rules relating masses (M_V, M_A) and decay constants (F_V, F_A) of vector and axial-vector resonances, they find that unitarity violation can be delayed to as much as 3.7 TeV for $M_A = 1.5$ TeV. However, there is a critical value of the coupling $g \equiv 2M_V^2/F_V^2$ above which the theory violates unitarity at a much lower energy. Thus in the latter case, a spin-0 isospin-0 resonance would be required. On the other hand, for values of g below the critical value, the theory may very well be Higgsless. However, it is entirely possible that the resonance being heavy may be difficult to observe.

2.3. Beyond SM scenarios with a light Higgs

There are two categories of theories which can have a light Higgs boson, with new physics in WW scattering above the light Higgs resonance. The first category corresponds to multi-Higgs models, where more than one doublet of scalar fields is introduced. In such a case WW scattering amplitude would grow after crossing the light Higgs resonance, but it could remain weak, if the heavier Higgs lies below the unitarity limit [4, 5]. The other category corresponds to a scenario where there is one light Higgs boson, which is light because it is a pseudo-Goldstone boson corresponding to the breaking of a global symmetry. The Higgs could get mass only at the loop level. Above the light Higgs resonance, the WW scattering amplitude could be strong, and the resulting theory could have other resonances. The Little Higgs models, together with theories with holographic Higgs, are studied in [6] under the category of “strongly-interacting light Higgs” theories.

In such theories, the new sector responsible for electroweak symmetry breaking, characterized by two parameters, a coupling g_ρ and a scale m_ρ describing the mass of heavy physical states. The coupling g_ρ , while larger than a typical SM coupling, is restricted to be below 4π to ensure that loop expansion remains depend-

able.

Experimental tests of such models would be observation of new states in addition to the light Higgs boson. However, even in the absence of new states, $W_L W_L$ scattering amplitudes would be found to grow as E^2/f^2 , where $f \equiv m_\rho/g_\rho$, since the Higgs boson moderates the high-energy behaviour only partially. Thus a study of gauge-boson scattering would prove useful. It is also predicted that there would be strong double-Higgs production through $W_L W_L \rightarrow HH$.

2.4. Higgsless models

A number of Higgsless models have been proposed recently [25, 26]. In these models, symmetry breaking is achieved by appropriate boundary conditions. The models differ in spatial dimensions, 5 in the original versions, 4 in the “deconstructed” versions. They also differ in embedding of SM fermions.

A feature common to such theories in five dimensions is that new weakly coupled particles, *viz.*, the Kaluza-Klein excitations of the gauge bosons appear at TeV scale and cancel the bad high-energy behaviour of WW scattering amplitudes, and thus postpone unitarity violation. A version of the model with modified fermion sector can raise the scale of unitarity violation by at least a factor of 10 without running into conflict with precision electroweak constraints.

In the absence of Higgs, new massive vector boson (MVB) propagators contribute to WW scattering. The bad high energy behaviour of WZ scattering, for example, is cancelled by the contribution of the MVBs because of coupling constant sum rules [27]:

$$g_{WWZZ} = g_{WWZ}^2 + \sum_i (g_{WZV}^{(i)})^2, \quad (31)$$

$$2(g_{WWZZ} - g_{WWZ}^2)(M_W^2 + M_Z^2) + g_{WWZ}^2 \frac{M_Z^4}{M_W^2} \\ = \sum_i (g_{WZV}^{(i)})^2 \left[3(M_i^\pm)^2 - \frac{(M_Z^2 - M_W^2)^2}{(M_i^\pm)^2} \right]. \quad (32)$$

Unitarity is violated at a scale

$$\Lambda \approx \frac{3\pi^4}{g^2} \frac{M_W^2}{M_1^\pm} \approx 5 - 10 \text{ TeV}. \quad (33)$$

The first MVB should appear below 1 TeV, and thus accessible at LHC. In the approximation that the first state V_1 saturates the sum rules, its partial width is given by

$$\Gamma(V_1^\pm \rightarrow W^\pm Z) \approx \frac{\alpha(M_1^\pm)^3}{144s_W^2 M_W^2}. \quad (34)$$

For $M_1^\pm = 700 \text{ GeV}$, the width is about 15 GeV. In SM, there is no resonance in $W^\pm Z$ scattering

Even in Higgsless models, one has to distinguish between cases where $W_L W_L$ scattering is weak, and where it is strong. Thus, if the MVB’s are light, with mass below 1 TeV, gauge-boson scattering will be weak. However, if the MVB’s are far above 1 TeV in mass, $W_L W_L$ scattering will be strong [28].

We now look at the practical aspects of actual observation of WW scattering at the LHC.

3. WW scattering at LHC

At a hadron collider like the LHC, WW scattering can occur with virtual W ’s emitted by the quarks in the hadrons. A W pair in the final state can be produced either through WW scattering diagrams, or through W emission from the partons of the initial hadrons. Fig. 2 shows these two types of contributions. Fig. 2 (a) represents the genuine WW scattering diagrams, whereas Fig. 2 (b) shows the “Bremsstrahlung” diagrams, which would be a background in the study of WW scattering.

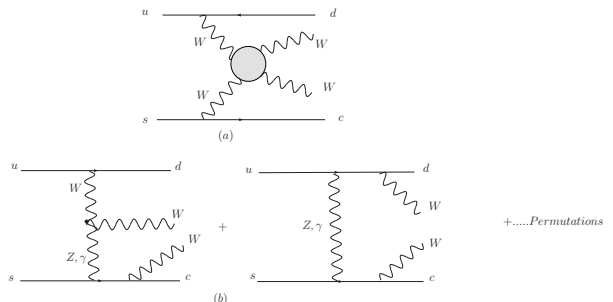


Figure 2. Main diagram topologies for the process $us \rightarrow cdW^+W^-$. (From [29]).

Thus, to study WW scattering at LHC, one has to find ways of separating the genuine scattering contribution from the other “Bremsstrahlung” contributions, which is no mean task. In fact, as we shall see, the interference between these two classes of diagrams is large, and huge cancellations can take place. Moreover, the gauge bosons taking part in the scattering are necessarily virtual (in fact, space-like). Thus the formalism has to take into account the virtuality of the gauge bosons.

A standard approach in the past to processes involving gauge bosons has been the equivalent vector-boson approximation, an extension of the equivalent-photon approximation used since early times [30].

3.1. Equivalent vector-boson approximation

The equivalent-photon approximation (Weizsäcker-Williams approximation) relates the cross section for a charged particle beam to interact with a target with a virtual photon exchange to the cross section for real photon beam to interact with the same target and produce the final state:

$$\sigma = \int dx \sigma_\gamma(x) f_{e/\gamma}(x). \quad (35)$$

Here, the photon distribution with momentum fraction x in a charged-particle beam of energy E is given by

$$f_{e/\gamma}(x) = \frac{\alpha}{2\pi x} \ln\left(\frac{E}{m_e}\right) [x + (1-x)^2]. \quad (36)$$

This is generalized to what is known as an equivalent (or effective) vector-boson approximation (EVBA) for a process with weak bosons in place of photons [31, 32]. The corresponding distributions of vector bosons V in a fermion f are given by [32]

$$\begin{aligned} f_{f/V_\pm}(x) &= \frac{\alpha}{2\pi x} \ln\left(\frac{E}{m_V}\right) \\ &\quad \times [(v_f \mp a_f)^2 + (1-x)^2(v_f \pm a_f)^2] \\ f_{f/V_L}(x) &= \frac{\alpha}{\pi x} (1-x) [v_f^2 + a_f^2]. \end{aligned} \quad (37)$$

Here the suffixes \pm on V denote the helicities ± 1 of V and V_L is the state with helicity 0.

The use of EVBA entails (a) restricting to vector boson scattering diagrams (b) neglecting diagrams of Bremsstrahlung type (c) putting on-shell momenta of the vector bosons which take part in the scattering and (d) approximating the total cross section of the process $f_1 f_2 \rightarrow f_3 f_4 V_3 V_4$ by the convolution of the vector boson luminosities $\mathcal{L}_{s_1 s_2}^{V_1 V_2}(x)$ with the on-shell cross section:

$$\begin{aligned} \sigma(f_1 f_2 \rightarrow f_3 f_4 V_3 V_4) &= \int dx \sum_{V_1, V_2} \sum_{s_1 s_2} \mathcal{L}_{s_1 s_2}^{V_1 V_2}(x) \\ &\quad \times \sigma_{s_1 s_2}^{on}(V_1 V_2 \rightarrow V_3 V_4, x s_{qq}) \end{aligned} \quad (38)$$

Here $x = M(V_1 V_2)^2 / s_{qq}$, while $M(V_1 V_2)$ is the vector boson pair invariant mass and s_{qq} is the square of the partonic c.m. energy, and s_1, s_2 are the spins of V_1, V_2 . Note in the context of (c) above that the on-shell point $q_{1,2}^2 = M_{V_{1,2}}^2$ is outside the physical region $q_{1,2}^2 \leq 0$. Thus the extrapolation involved is more than that involved in the case of the equivalent-photon approximation.

Even if only the longitudinal polarization, expected to be dominant, is kept, EVBA overestimates the true cross section. The transverse polarization contribution is found to be comparable to the longitudinal one [32].

Improved EVBA [33], going beyond the leading approximation, still overestimates the cross section [34]. Further improvements in EVBA have been attempted [35].

3.2. Backgrounds

Backgrounds are of two types:

1. Bremsstrahlung processes – these are processes where the vector bosons are radiated by quark or anti-quark partons, and which do not contribute to VV scattering.

2. Processes which fake a VV final state.

It is important to understand the first inherent background, and device cuts which may enhance the signal. However, it may be possible to live with it – provided VV scattering signal is anyway enhanced because it is strong. In that case, one simply makes predictions for the combined process of $PP \rightarrow VV + X$. The second background is crucial to take care of, otherwise we do not know if we are seeing a VV pair in the final state or not.

Background processes are $q\bar{q} \rightarrow W^+W^-X$, $gg \rightarrow W^+W^-X$, $t\bar{t} + \text{jet}$, with top decays giving W^+W^- pair. Electroweak-QCD process $W^+ + \text{jets}$ can mimic the signal when the invariant mass of the two jets is around m_W . There is a potential background from QCD processes $q\bar{q}, gg \rightarrow t\bar{t}X, Wt\bar{b}$ and $(t\bar{t} + \text{jets})$, in which a W can come from the decay of t or \bar{t} . W boson pairs produced from the intrinsic electroweak process $q\bar{q} \rightarrow q\bar{q}W^+W^-$ tend to be transversely polarized. Coupling to W^+ of incoming quark is purely left-handed. Helicity conservation implies that outgoing quark follows the direction of incoming quark for longitudinal W , and it goes opposite to direction of incoming quark for transverse (left-handed) W . Hence outgoing quark jet is less forward in background than in signal event, and tagging of the forward jet can help.

In addition, emission in the central region is favoured in the QCD background processes, whereas jet production in the central region is suppressed for WW scattering. Thus, a veto on additional jets in the central region would be a powerful discriminant between signal and background.

For a discussion of the WW scattering in the context of LHC detectors, see [36].

3.3. Distinguishing the signal

The feasibility of extracting WW scattering from experiment and comparison of EVBA with exact results was recently studied by Accomando and collaborators [29].

It is known that when W 's are allowed to be off mass

shell, the amplitude grows faster with energy, as compared to when they are on shell [37]. The problem of bad high-energy behaviour of WW scattering diagrams can be avoided by the use of the axial gauge [38].

Accomando *et al.* [29] have examined (a) the role of choice of gauge in WW fusion, in particular, the axial gauge, (b) the reliability of EVBA, (c) the determination of regions of phase space, in suitable gauge, which are dominated by the signal (i.e., the WW scattering diagrams). Their results show that WW scattering diagrams do not constitute the dominant contribution in any gauge or phase space region. Thus, there is no substitute to the complete amplitude for studying WW fusion process at LHC.

A similar discussion in the context of the EWCL including resonances, in contrast to the discussion of Accomando *et al.*, is found in [18], where again the predictions of EVBA are compared with those obtained from the event generator WHIZARD.

We now describe some of the results of [29].

Table 1 shows the cross section in different gauges for the contribution of us partons to the full process $pp \rightarrow W^+W^-X$, to only the WW diagrams, and the ratio of these cross sections. The Higgs boson mass is assumed to be 200 GeV, and a cut on the WW invariant mass $M(WW)$ of 300 GeV is applied. It is clear that in the WW contribution is largely cancelled by the ‘‘Bremsstrahlung’’ type background contribution. Even in the axial gauge, in which the WW contribution is the least, it is still a factor of 2 larger than the actual cross section.

Table 1. Contribution to the cross section from WW diagrams and all diagrams for Higgs mass of $M_H = 200$ GeV and $M(WW) > 300$ GeV. Also shown is the ratio of the WW contribution to the total contribution. (From [29]).

Gauge	$\sigma(pb)$		Ratio WW/all
	All diagrams	WW diagrams	
Unitary	$8.50 \cdot 10^{-3}$	6.5	765
Feynman	$8.50 \cdot 10^{-3}$	0.221	26
Axial	$8.50 \cdot 10^{-3}$	$2.0 \cdot 10^{-2}$	2.3

WW invariant-mass distributions are also obtained in [29]. Again, the result including all diagrams does not give a true representation of the WW contribution alone. Accomando *et al.* have also made a comparison

of the WW invariant mass distribution for the process $us \rightarrow dcW^+W^-$ in an improved EVBA with the exact complete result for the two cases of a very heavy Higgs and a Higgs of mass 250 GeV. EVBA exceeds the exact result except at the Higgs resonance. Ref. [29] also investigated the total cross section in EVBA and exact computation and their ratio for different cuts on the W scattering angle. The angular cuts serve to decrease the discrepancy between EVBA and exact computation.

The WW invariant mass distribution in the process $PP \rightarrow us \rightarrow cdW^+W^-$ is shown in Fig. 3.3, imposing the cuts $E(\text{quarks}) > 20$ GeV, $p_T(\text{quarks}, W) > 10$ GeV, $2 < |\eta(\text{quark})| < 6.5$, $|\eta(W)| < 3$. It is seen that for sufficiently large WW invariant mass it seems feasible to distinguish between light Higgs and heavy Higgs scenarios. It is reasonable to anticipate that this is the kinematic region where it may be possible to test non-standard scenarios of symmetry breaking.

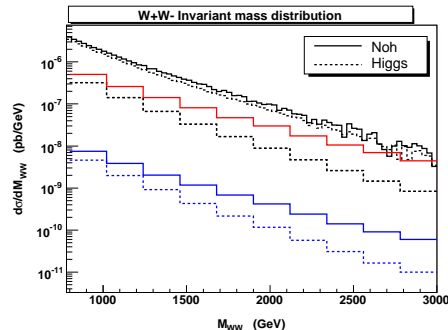


Figure 3. The WW invariant mass distribution in $PP \rightarrow us \rightarrow cdW^+W^-$ for no Higgs (solid curves) and for $M_h = 200$ GeV (dashed curve). The two intermediate (red) curves are obtained imposing cuts shown below. The two lowest (blue) curves refer to the process $PP \rightarrow us \rightarrow cd\mu^- \bar{\nu}_\mu e^+ \nu_e$ with further acceptance cuts: $E_l > 20$ GeV, $p_T^\ell > 10$ GeV, $|\eta_l| < 3$.

While the study of Accomando *et al.* is revealing, it may be argued that the alternative to SM with a light Higgs boson that they consider is a somewhat *ad hoc* and unphysical $m_H \rightarrow \infty$ limit of SM. In that context, the study carried out by Éboli, Gonzalez-Garcia and Mizukoshi [17] in the framework of EWCL may be considered more systematic. They impose jet acceptance cuts of $p_T^j > 20$ GeV, $|\eta_j| < 4.9$, and demand a rapidity gap between jets through $|\eta_{j1} - \eta_{j2}| > 3.8$, $\eta_{j1} \cdot \eta_{j2} < 0$. The lepton acceptance and isolation cuts used are $|\eta_\ell| < 2.5$, $\eta_{\min}^j < \eta_\ell < \eta_{\max}^j$, with $\eta_{\min(\max)}^j$ as the minimum (maximum) rapidity of the tagging

jets, $\Delta R_{\ell j} \geq 0.4$, $\Delta R_{\ell\ell} \geq 0.4$, and $p_T^\ell \geq p_T^{\min}$, where $p_T^{\min} = 100(30)$ GeV for opposite(equal) charge leptons. Since signal events contain neutrinos, they also require a missing transverse momentum $p_T^{\text{missing}} \geq 30$ GeV. In addition, to suppress the SM background as well as background from $t\bar{t}$ production, they impose additional cuts on the invariant masses of the pair of tagging jets, and of the W pair. We refer to the original paper for the details. However, here we limit ourselves to pointing out the sensitivity they obtain, *viz.*, eq. (27).

The results on the sensitivity obtained in ref. [17] were made use of in [15] to discuss the feasibility of observation of two scenarios of SSB in the context of EWCL. One of these is the heavy Higgs scenario, where the Higgs mass is assumed to be between 2 and 2.5 TeV. While perturbative calculations are not reliable for such Higgs masses, it is presumed that some insight would be obtained into the strongly interacting behaviour. A calculation of the EWCL coefficients in this case yields values which, using eq. (27), are too small to be observable at LHC. A similar conclusion has been drawn in a generic technicolor type of model in the large N limit for an $SU(N)$ gauge theory for confinement of technifermions.

It seems that the prospects for the observation of non-trivial effects in WW scattering are limited to vector and scalar resonances, whatever the dynamics that produce the resonances. A concrete study in the context of EWCL with extra resonances is [18] and in the context of Higgsless models can be found in [39].

4. Discussion

In the absence of a light Higgs, WW interactions become strong at TeV scales leading to violation of perturbative unitarity. Study of WW scattering can give information of the electroweak symmetry breaking sector and discriminate between models.

There are a number of possible scenarios. In the standard model with a light Higgs boson ($m_H \lesssim 1$ TeV), WW scattering is well-behaved at large energies. On the other hand, if the SM Higgs boson is heavier than about 1 TeV, WW interactions become strong. For extensions of SM, there are various possibilities. One possibility is that there are no elementary scalars, and SSB is dynamical in origin. In that case, WW scattering would show new features which restore unitarity, possibly resonances. In theories with extra dimensions like Higgsless models, the violation of unitarity is delayed to higher energies because of the cancellation of the leading high-energy term by the exchange of Kaluza-Klein excitations of gauge bosons, which would be seen as res-

onances. A further possibility is that there is a light Higgs boson, which postpones unitarity violation, but there is new physics beyond. The new physics in its simplest form could be extra Higgs, and WW scattering could be weak or strong depending on the masses of these Higgs bosons. A more sophisticated possibility is that the light Higgs is a pseudo-Goldstone boson of some higher symmetry, and the WW scattering above the Higgs resonance would show interesting features. Thus WW scattering needs to be studied even if a light Higgs boson is found.

New physics could be modelled by means of an effective theory valid at low energies, *viz.*, EWCL, whose lowest dimensional operators would be fixed by the low-energy theorems, but operators with higher dimensions would have coefficients fixed either from experiment, or on the basis of a detailed theory which describes the ultra-violet sector completely. Such a formalism has to be combined with a suitable method of unitarization.

Two of the coefficients of higher dimensions are constrained by precision experiments. Two others would be constrained by the four-point couplings of the gauge bosons. Studies of popular scenarios of SSB beyond SM show that a determination of these latter couplings may pose a challenge to LHC.

In general there are large cancellations between the scattering and Bremsstrahlung diagrams. Hence extraction of WW scattering contribution from the process $PP \rightarrow W^+W^-X$ needs considerable effort. EVBA overestimates the magnitude in most kinematic distributions. Appropriate cuts to reduce background are most essential. It is possible to extract information on WW scattering from hadronic experiments by concentrating on the large-invariant mass region.

Acknowledgements I thank Andreas Nyffeler for comments and discussions. I also thank Namit Mahajan for discussions and pointing out ref. [10].

REFERENCES

1. J. M. Cornwall, D. N. Levin and G. Tiktopoulos, *Phys. Rev. D* **10** (1974) 1145, *ibid.* **11** (1975) 972 (E); C. E. Vayonakis, *Lett. Nuovo Cim.* **17** (1976) 383; B. W. Lee, C. Quigg and H. B. Thacker, *Phys. Rev. D* **16** (1977) 1519; D. A. Dicus and V. S. Mathur, *Phys. Rev. D* **7** (1973) 3111; M. S. Chanowitz and M. K. Gaillard, *Nucl. Phys. B* **261** (1985) 379; H. G. J. Veltman, *Phys. Rev. D* **41** (1990) 2294. G. Gounaris, R. Kögerler, and H. Neufeld, *Phys. Rev. D* **34**, 3257(1986); J. Bagger and C. Schmidt, *Phys. Rev. D* **41**, 264 (1990); W. Kilgore, *Phys. Lett. B* **294**, 257 (1992); H-J. He,

- Y-P. Kuang, X-Y. Li, *Phys. Rev. Lett.* **69**, 2619 (1992); *Phys. Rev. D* **49**, 4842 (1994); H-J. He and W. Kilgore, *Phys. Rev. D* **55**, 1515 (1997) [arXiv:hep-ph/9609326].
2. S. Weinberg, *Phys. Rev.* **166** (1968) 1568.
 3. M. E. Peskin and T. Takeuchi, *Phys. Rev. D* **46**, 381 (1992); *Phys. Rev. Lett.* **65**, 964 (1990).
 4. K. Cheung, C. W. Chiang and T. C. Yuan, arXiv:0803.2661 [hep-ph].
 5. L. Randall, *JHEP* **0802** (2008) 084 [arXiv:0711.4360 [hep-ph]].
 6. G. F. Giudice, C. Grojean, A. Pomarol and R. Rattazzi, *JHEP* **0706** (2007) 045 [arXiv:hep-ph/0703164].
 7. T. Appelquist and C. W. Bernard, *Phys. Rev. D* **22** (1980) 200; A. C. Longhitano, *Nucl. Phys. B* **188** (1981) 118; *Phys. Rev. D* **22** (1980) 11; T. Appelquist and G. H. Wu, *Phys. Rev. D* **48** (1993) 3235 [arXiv:hep-ph/9304240].
 8. A. Dobado, M. J. Herrero and J. Terron, *Z. Phys. C* **50** (1991) 205;
 9. G. F. Chew and S. Mandelstam, *Phys. Rev.* **119**, 467 (1960).
 10. J. A. Oller, *Phys. Lett. B* **477**, 187 (2000) [arXiv:hep-ph/9908493]; K. i. Hikasa and K. Igi, *Phys. Rev. D* **48** (1993) 3055; *Phys. Lett. B* **261** (1991) 285 [Erratum-ibid. **270** (1991) 128].
 11. J. A. Bagger, A. F. Falk and M. Swartz, *Phys. Rev. Lett.* **84** (2000) 1385 [arXiv:hep-ph/9908327].
 12. J. Distler, B. Grinstein, R. A. Porto and I. Z. Rothstein, *Phys. Rev. Lett.* **98** (2007) 041601 [arXiv:hep-ph/0604255].
 13. L. Vecchi, *JHEP* **0711** (2007) 054 [arXiv:0704.1900 [hep-ph]].
 14. T. N. Pham and T. N. Truong, *Phys. Rev. D* **31**, 3027 (1985); B. Ananthanarayan, D. Toublan and G. Wanders, *Phys. Rev. D* **51**, 1093 (1995) [arXiv:hep-ph/9410302]; M. R. Pennington and J. Portoles, *Phys. Lett. B* **344**, 399 (1995) [arXiv:hep-ph/9409426].
 15. M. Fabbrichesi and L. Vecchi, *Phys. Rev. D* **76**, 056002 (2007) [arXiv:hep-ph/0703236].
 16. A. S. Belyaev, O. J. P. Éboli, M. C. Gonzalez-Garcia, J. K. Mizukoshi, S. F. Novaes and I. Zacharov, *Phys. Rev. D* **59** (1999) 015022 (1999) [arXiv:hep-ph/9805229].
 17. O. J. P. Éboli, M. C. Gonzalez-Garcia and J. K. Mizukoshi, *Phys. Rev. D* **74** (2006) 073005 [arXiv:hep-ph/0606118].
 18. A. Alboteanu, W. Kilian and J. Reuter, arXiv:0806.4145 [hep-ph].
 19. W. Kilian, T. Ohl and J. Reuter, arXiv:0708.4233 [hep-ph]; T. Ohl, AIP Conf. Proc. **583**, 173 (2001) [arXiv:hep-ph/0011243]; M. Moretti, T. Ohl and J. Reuter, arXiv:hep-ph/0102195; J. Reuter, arXiv:hep-th/0212154.
 20. S. Weinberg, *Phys. Rev. D* **19**, 1277 (1979); L. Susskind, *Phys. Rev. D* **20**, 2619 (1979).
 21. S. Dimopoulos and L. Susskind, *Nucl. Phys. B* **155**, 237 (1979); E. Eichten and K. D. Lane, *Phys. Lett. B* **90** (1980) 125.
 22. B. Holdom, *Phys. Rev. D* **24**, 1441 (1981); E. Eichten and K. D. Lane, *Phys. Lett. B* **90**, 125 (1980); K. D. Lane and E. Eichten, *Phys. Lett. B* **222**, 274 (1989).
 23. R. Foadi, M. T. Frandsen and F. Sannino, *Phys. Rev. D* **77**, 097702 (2008) [arXiv:0712.1948 [hep-ph]]; R. Foadi, M. T. Frandsen, T. A. Ryttov and F. Sannino, *Phys. Rev. D* **76**, 055005 (2007) [arXiv:0706.1696 [hep-ph]]; D. D. Dietrich, F. Sannino and K. Tuominen, *Phys. Rev. D* **73**, 037701 (2006) [arXiv:hep-ph/0510217].
 24. R. Foadi and F. Sannino, arXiv:0801.0663 [hep-ph].
 25. C. Csaki, C. Grojean, H. Murayama, L. Pilo and J. Terning, *Phys. Rev. D* **69** (2004) 70 [hep-ph/0305237]; C. Csaki, C. Grojean, L. Pilo and J. Terning, *Phys. Rev. Lett.* **92** (2004) 101802 [hep-ph/0308038].
 26. Y. Nomura, *JHEP* **11** (2003) 050 [arXiv:hep-ph/0309189].
 27. A. Birkedal, K. Matchev and M. Perelstein, *Phys. Rev. Lett.* **94** (2005) 191803 [hep-ph/0412278].
 28. M. S. Chanowitz, *Czech. J. Phys.* **55** (2005) B45 [arXiv:hep-ph/0412203].
 29. E. Accomando, A. Ballestrero, A. Belhouari and E. Maina, *Phys. Rev. D* **74** (2006) 073010 [arXiv:hep-ph/0608019].
 30. E. Fermi *Z. Phys.* **29** (1924) 315; C. F. von Weizsacker, *Z. Phys.* **88** (1934) 612; E. J. Williams, *Phys. Rev. D* **45** (1934) 729.
 31. S. Dawson, *Nucl. Phys. B* **249** (1985) 42; G. L. Kane, W. W. Repko and W. B. Rolnick, *Phys. Lett. B* **148** (1984) 367; J. Lindfors, *Z. Phys. C* **28** (1985) 427.
 32. R. M. Godbole and S. D. Rindani, *Phys. Lett. B* **190** (1987) 192; *Zeit. Phys. C* **36** (1987) 395.
 33. P. W. Johnson, F. I. Olness, and W.-K. Tung, *Phys. Rev. D* **36** (1987) 291.
 34. R. M. Godbole and F. I. Olness, *Int. J. Mod. Phys. A* **2** (1987) 1025.
 35. I. Kuss and H. Spiesberger, *Phys. Rev. D* **53** (1996) 6078 [arXiv:hep-ph/9507204].
 36. ATLAS Collaboration, CERN/LHCC/99-15; CMS Collaboration, CERN/LHCC/94-38.

37. R. Kleiss and W. J. Stirling, *Phys. Lett. B* **182** (1986) 75.
38. Z. Kunszt and D. E. Soper, *Nucl. Phys. B* **296** (1988) 253.
39. R. Malhotra, hep-ph/0611380.